Inorg. Chem. **1991**, *30*, 528-535

Contribution from the Department of Chemistry,
University of California, Davis, California 95616

Synthesis and Structure of Diarylboryl-Substituted Hydrazines and Diphosphanes:† Role of σ-Orbital Hybridization and π-Orbital Overlap in N–N and P–P Multiple-Bond Lengths

Doris C. Pestana and Philip P. Power*

Received July 3, 1990

The synthesis and spectroscopic and structural characterization of several substituted diphosphanes and hydrazines have been carried out in order to estimate the relative importance of rehybridization and π-bonding in N–N and P–P double-bond lengths. The presence of the $-BMes_2$ (Mes = 2,4,6-$Me_3C_6H_2$) group in the compounds $Mes_2B(1\text{-}Ad)PPPh_2$ (**1**) (1-Ad = 1-adamantyl), $[Mes_2B(1\text{-}Ad)P]_2$ (**2**), and $[Mes_2B(Mes)P]_2$ (**3**) induces essential planarity at the boryl-substituted phosphorus atoms and dramatic changes in the P–P bond lengths. Normally, single P–P bonds are about 2.22 Å long, as is observed in $[Mes(I)P]_2$ (**4**), whereas in **1** the P–P bond length is near 2.17 Å and in **2** and **3** it is near 2.11 Å. The latter distance is about halfway between those of normal single and double P–P bonds. The use of the $-BMes_2$ group as a substituent on hydrazines also results in planarity at the boryl-substituted nitrogen and in the shortening of the N–N bonds. In this case, however, the percentage change in the N–N bond length is not as great as that seen in the phosphorus compounds. For example, the N–N bond length in $Mes_2B(Ph)NN(H)Ph$ (**5**) is near 1.44 Å and in $Mes_2B(H)NN(H)BMes_2$ (**6**) it is 1.41 Å whereas in hydrazine the N–N distance is 1.46 Å (cf. N–N double bond ≈ 1.25 Å). Oddly, the N–N bond length in 1,2-diphenylhydrazine (**7**) is 1.39 Å. In this case, however, the nitrogen is almost planar and the N–C bond is short. The larger changes observed in the diphosphanes have been interpreted on the basis of the relative weakness of the P–P π-bond and the fact that the hybridization changes in phosphorus are significantly greater than those observed for nitrogen. Similarly, comparison of the data for **1**–**7** with the normal bond lengths for P–P and N–N double bonds, which are 2.02 and 1.25 Å long, respectively, leads to the conclusion that p–p π-bonds account for only about half of the shortening in P–P double bonds whereas they account for ~70–75% of the contraction in the case of N–N double bonds.

Introduction

One of the most exciting recent developments in main-group chemistry has been the synthesis and structural characterization of a wide variety of compounds that contain multiple bonds between the heavier elements.[1] This has led to the virtual overthrow of the so-called "double-bond rule".[2] This revolution has progressed to the extent that it is now widely believed that, within the restrictions imposed by valency requirements, it should be possible to prepare compounds having multiple bonds between any given pair of heavy main-group elements.[3]

In much of the work published to date, bond lengths have been used as the primary index of multiple bonding. For example, phosphorus–phosphorus double bonds are within the range 2.0–2.05 Å[1c,3a,4] and are roughly 8–10% shorter than a typical phosphorus–phosphorus single bond of length 2.22 Å.[5] The corresponding lengths for Si–Si single and double bonds are 2.36 and 2.14 Å.[1b,3b] Moreover, the shortening in the double bonds is often assumed to be due mainly to the addition of a π-interaction as a result of overlap of adjacent p orbitals. This reasoning has its origins in carbon chemistry, where the classical model for the double bond (in ethylene, for example) comprises a single σ-bond, arising from overlap of sp^2 hybrid orbitals from carbon, and a π-bond arising from the overlap of the remaining p orbitals. It has been realized for many years that the change in hybridization at carbon ($sp^3 \rightarrow sp^2$) also contributed to the shortening observed for the double bond.[6] Comparison of C–C bond lengths in a variety of compounds has led to the conclusion that ~25–30% of the observed contraction could be attributed to rehybridization.[6] One of the major questions that the work described in this paper attempts to answer concerns the relative contribution of rehybridization to the bond contraction in related compounds that involve multiple bonds between the pairs of atoms N–N and P–P. The compounds $Mes_2B(1\text{-}Ad)PPPh_2$ (**1**), $[Mes_2B(1\text{-}Ad)P]_2$ (**2**), $[Mes_2B(Mes)P]_2$ (**3**), $[Mes(I)P]_2$ (**4**), $Mes_2B(Ph)N(H)Ph$ (**5**), and $[Mes_2B(H)N]_2$ (**6**) have been synthesized and characterized in order to probe the effects of rehybridization on their N–N and P–P bond lengths. The structure of $[Ph(H)N]_2$ (**7**) has also been determined in order to provide data for comparison purposes.

Experimental Section

General Procedures. All manipulations were performed either by using modified Schlenk techniques or a Vacuum Atmospheres HE 43-drybox with a N_2 atmosphere. Solvents were freshly distilled from Na/K alloy or Na/K alloy–benzophenone ketyl and degassed twice immediately before use. ^{31}P, ^{11}B, and ^1H NMR spectra were recorded in C_6D_6 solutions by using a General Electric QE-300 spectrometer operating at 121.70, 96.46, or 300.66 MHz, respectively. ^{31}P and ^{11}B NMR spectra were referenced to external 85% H_3PO_4 and $BF_3{\cdot}Et_2O$ standards. Ph_2PCl, I_2, dry NH_2NH_2, 1,2-diphenylhydrazine, and *n*-BuLi 1.6 M in hexane were obtained commercially and used as received. 1-$AdPH_2$[7] and Mes_2BF[8] were prepared according to literature methods. Crystals of 1,2-diphenylhydrazine that were adequate for X-ray structure determination were obtained by recrystallization of a commercial sample from hexane. NEt_3 was distilled under N_2 from P_2O_5 and degassed twice before use. All compounds gave a satisfactory C and H (and N where appropriate) analysis.

$Mes_2B(1\text{-}Ad)PPPh_2$ (1). *n*-BuLi (1.6 M, 3.7 mL, 5.9 mmol) was added slowly to a solution of 1-$AdPH_2$ (0.98 g, 5.8 mmol) in Et_2O (45 mL) with cooling in an ice bath. The resulting yellow solution was stirred for 0.5 h at 0 °C and allowed to reach room temperature, whereupon stirring was continued for 1 h. Cooling again in an ice bath and the addition of a solution of Mes_2BF (1.57 g, 5.85 mmol) in Et_2O (45 mL) gave a dark orange-brown suspension upon stirring for 12 h at room temperature. With cooling in an ice bath, another equivalent of *n*-BuLi was added. This yielded a brighter orange solution upon stirring for 2 h. Ph_2PCl (1.32 g, 5.98 mmol) in Et_2O (35 mL) was then added drop-

---

† The term diphosphane, which is used here for H_2PPH_2 and its derivatives, is preferred to diphosphine owing to the possible confusion arising from the similarity in pronunciation of the latter name to that of diphosphene.

(1) For example: (a) Goldberg, D. E.; Harris, D. H.; Lappert, M. F.; Thomas, K. M. *J. Chem. Soc., Chem. Commun.* **1976**, 261 (Sn–Sn double bonds). (b) West, R.; Fink, M. J.; Michl, T. *Science (Washington D.C.)* **1981**, *214*, 1343 (Si–Si double bonds). (c) Yoshifuji, M.; Shima, I.; Inamoto, N.; Hirotsu, K.; Higuchi, T. *J. Am. Chem. Soc.* **1981**, *103*, 4587 (P–P double bonds).

(2) Jutzi, P. *Angew. Chem., Int. Ed. Engl.* **1975**, *14*, 32. Gusel'nikov, L. E.; Nametkin, N. S. *Chem. Rev.* **1979**, *79*, 529.

(3) Reviews: (a) Cowley, A. H.; Norman, N. C. *Prog. Inorg. Chem.* **1986**, *34*, 1. (b) West, R. *Angew. Chem., Int. Ed. Engl.* **1987**, *26*, 1201.

(4) Cowley, A. H. *Polyhedron* **1984**, *3*, 389; *Acc. Chem. Res.* **1984**, *17*, 386.

(5) Corbridge, D. E. *The Structural Chemistry of Phosphorus*; Elsevier: Amsterdam, 1976, p 393.

(6) March, J. *Advanced Organic Chemistry*, 3rd ed.; Wiley: New York, 1985; 18–19 and references therein.

(7) Stetter, H.; Last, W. *Chem. Ber.* **1969**, *102*, 3364.

(8) We thank Professor A. Pelter for a high-yield synthesis of Mes_2BF when the published procedure did not work in our hands. The method of synthesis is identical with that described for $(2,6\text{-}Me_2C_6H_3)_2BF$: Chen, H.; Bartlett, R. A.; Olmstead, M. M.; Shoner, S. C. *J. Am. Chem. Soc.* **1990**, *112*, 1048.

0020-1669/91/1330-0528$02.50/0

Table I. Crystallographic Data for Compounds **1** and **4–7**

	Mes$_2$B(1-Ad)PPPh$_2$ (**1**)	[Mes(I)P]$_2$ (**4**)	Mes$_2$B(Ph)NN(Ph)H (**5**)	Mes$_2$B(H)NN-(H)BMes$_2$ (**6**)	[Ph(H)N]$_2$ (**7**)
formula	$C_{40}H_{47}BP_2$	$C_{18}H_{22}P_2I_2$	$C_{30}H_{33}BN_2$	$C_{36}H_{46}B_2N_2$	$C_{12}H_{12}N_2$
a, Å	10.593 (4)	8.119 (2)	14.267 (4)	15.884 (7)	19.652 (8)
b, Å	20.313 (10)	16.322 (4)	10.969 (2)	13.240 (2)	7.353 (2)
c, Å	16.017 (7)	8.352 (2)	16.833 (5)	15.655 (3)	7.492 (2)
β, deg	103.57 (3)	115.76 (2)	108.85 (2)	105.77 (2)	110.70 (3)
V, Å^3	3350.2 (26)	996.8 (4)	2493.0 (10)	3168.4 (15)	1012.7 (6)
Z	4	2 (dimers)	4 (dimers)	4 (dimers)	4 (dimers)
fw	600.57	554.12	432.41	528.39	184.24
space group (No.)	$P2_1/c$ (14)	$P2_1/a$ (14)	$P2_1/c$ (14)	$C2/c$ (15)	$C2/c$ (15)
T, K	130	130	130	130	130
λ, Å	0.71069	0.71069	0.71069	0.71069	0.71069
d(calc), g cm^{-3}	1.19	1.85	1.15	1.11	1.21
μ, cm^{-1}	1.52	32.75	0.62	0.58	0.68
transm coeff	0.95, 0.88	0.89, 0.63	0.98, 0.97	0.99, 0.97	1.00, 1.00
$R(F)$	0.0669	0.0354	0.0433	0.0524	0.0755
$R_w(F)$	0.0636	0.0400	0.0457	0.0865	0.0775

wise. The addition was accompanied by a color change to yellow and the appearance of a copious white precipitate. The mixture was then stirred overnight. All the volatile material was pumped off, and the yellow residue was extracted with 3 × 40 mL of pentane, giving an orange solution after filtration. Reduction of the volume to ~35 mL, under reduced pressure, produced incipient crystallization, and rewarming gave a clear solution, which was cooled in a 4 °C refrigerator overnight to afford **1** as yellow plates suitable for X-ray structure determination. Further cooling to −16 °C afforded a total yield of 1.25 g (36%). Mp = 167–171 °C. ^{1}H NMR (δ): 7.70, 6.95 (2 m, phenyl H); 6.76, 6.47 (2 s, *m*-H); 2.60, 2.45 (2 s, *o*-Me); 2.12 (m, 6 H of adamantyl and 1 *p*-Me); 2.03 (*p*-Me); 1.67 (br s, bridgehead adamantyl); 1.46 (br m, 6 H of adamantyl). ^{11}B NMR (δ): 72.3. ^{31}P NMR (δ): −19.75, 19.55 (J_{PP} = 316.5 Hz).

[Mes$_2$B(1-Ad)P]$_2$ (2). The synthesis of this compound has been outlined in a preliminary communication.[9] Mes$_2$BP(1-Ad)Li(Et$_2$O)$_2$ (1.02 g, 1.79 mmol) in THF (35 mL) was added dropwise at 0 °C to a suspension of CrCl$_3$ (0.26 g, 1.80 mmol) in THF (30 mL). The reaction mixture was allowed to warm to room temperature and stirred overnight. All volatile material was removed under reduced pressure and the brown-green residue taken up in pentane (~150 mL). Filtration through Celite gave an intensely colored yellow solution and a green-gray solid residue on the filter. Partial reduction of volume to ~85 mL, followed by slow cooling in a −20 °C freezer, produced dark yellow crystals of **2**, suitable for X-ray structure determination. Further volume reduction, ~15 mL, gave a total yield of 0.41 g (48%). Mp = 323–325 °C dec. ^{1}H NMR (δ): 6.73, 6.64 (2 s, 2 H each, *m*-H); 2.34, 1.98, 1.87 (br s, adamantyl); 2.23, 2.17, 1.55, 1.51 (s, *o*- and *p*-Me). ^{11}B NMR (δ): 52.8. ^{31}P NMR (δ): 2.8.

[Mes$_2$B(Mes)P]$_2$ (3). Mes$_2$BP(Mes)Li(Et$_2$O) (1.78 g, 3.59 mmol) in THF (25 mL) was added dropwise at 0 °C to a suspension of CrCl$_3$ (0.20 g, 1.26 mmol) in THF (40 mL). The reaction mixture was allowed to warm to room temperature and stirred overnight. All volatiles were removed under pressure; the olive green residue was taken up in toluene (80 mL), and the solution was filtered. Crystals of **3** for X-ray structure determination were grown from an ether solution (5 mL). Yield: 0.33 g (23%). Mp = 247–250 °C dec. ^{1}H NMR (δ): 6.6 (br s, *m*-H); 3.2 (q), 1.05 (t) (ethers of crystallization); 2.25, 2.07, 1.85 (br s, *o*- and *p*-Me). ^{11}B NMR (δ): 54.0. ^{31}P NMR (δ): −22.3.

[Mes(I)P]$_2$ (4). Mes$_2$BPMesLi(Et$_2$O)$_2$ (1.0 g, 1.80 mmol) was dissolved in Et$_2$O (35 mL), and the mixture was cooled in an ice bath. Iodine (0.46 g, 1.81 mmol) in Et$_2$O (40 mL) was added dropwise, and its brown color was discharged immediately. Stirring for 4 h at room temperature gave an orange-yellow solution. All volatile materials were then pumped off, and the dark yellow-orange residue was taken up in hexane (~45 mL); the solution was filtered twice and reduced in volume to ~5 mL. Cooling overnight at 0 °C gave a mixture of dark orange crystals of **4** and colorless Mes$_2$BI crystals adequate for X-ray structure determination. Further cooling to −16 °C afforded 0.05 g of **4** (10% yield). Mp = 187–191 °C. ^{31}P NMR (δ): 29.9. Mes$_2$BI melts at 99–103 °C. ^{1}H NMR (δ): 6.73 (s, 4 *m*-H); 2.26 (s, 4 *o*-Me); 2.14 (s, 2 *p*-Me). ^{11}B NMR (δ): 50.0.

Mes$_2$B(Ph)NN(H)Ph (5). 1,2-Diphenylhydrazine (0.92 g, 4.99 mmol) was dissolved in Et$_2$O (35 mL), and the mixture was cooled to ~0 °C in an ice bath. *n*-BuLi (1.6 M, 6.3 mL, 10.1 mmol) was added slowly over a period of 15 min. The solution was allowed to reach ambient temperature and refluxed for 1 h. Mes$_2$BF (2.66 g, 9.92 mmol) dissolved in Et$_2$O (25 mL) was then added dropwise. The reaction mixture was stirred for 45 min at room temperature and brought under reflux for 2 h. All the volatile material was pumped off, and the residue was taken up in hexane; the solution was filtered and reduced in volume to incipient crystallization (35 mL). Cooling to −16 °C afforded the product **5** as small colorless crystals, 1.10 g (51% yield). Mp = 199–202 °C. Crystals adequate for X-ray structure determination were obtained by recrystallization from ether. ^{1}H NMR (δ): 6.72, 6.71 (2 s, *m*-H); 7.30, 6.91, 6.64, 6.60 (4 m, phenyl H); 6.09 (s, NH); 2.25; 2.22 (2 s, *o*-Me); 2.09, 2.07 (2 s, *p*-Me). ^{11}B NMR (δ): 50.2.

[Mes$_2$B(H)N]$_2$ (6). Hydrazine (0.15 g, 4.68 mmol) was dissolved in hexane (25 mL), and NEt$_3$ (1.8 mL, 1.31 g, 12.9 mmol) was added. Mes$_2$BF (2.51 g, 9.36 mmol) dissolved in hexane (50 mL) was added dropwise to the N$_2$H$_4$/NEt$_3$ solution at room temperature. A white precipitate was observed almost immediately. The solution was stirred for 0.5 h at room temperature and refluxed for 1.5 h, whereupon all the white precipitate dissolved. Cooling to room temperature caused reprecipitation. After the volume of the solution was reduced to ~40 mL, the solution was filtered and further reduced in volume to ~20 mL. Cooling to 0 °C yielded colorless crystals of the product **6** that were adequate for X-ray structure determination. Yield: 1.25 g (51%). Mp = 217–219 °C. ^{1}H NMR (δ): 7.02 (s, NH); 6.73, 6.64 (2 s, *m*-H); 2.35, 2.20 (2 s, *o*-Me); 2.13, 2.04 (2 s, *p*-Me). ^{11}B NMR (δ): 38.8.

X-ray Crystallographic Studies. The X-ray data for compounds **1**, **4**, and **5** were collected by using a Syntex P2$_1$ diffractometer equipped with a locally modified Syntex LT-1 device. Calculations were carried out on a Data General Eclipse computer using a SHELXTL program system, Version 5. A Siemens R3 m/V diffractometer equipped with a locally modified Enraf-Nonius LT apparatus was employed for data collection of compounds **6** and **7**; calculations for the latter were carried out on a Micro VAX II computer using a SHELXTL PLUS program system. The atom form factors, including anomalous scattering, were from Ref 10.

Crystals of **1** and **4–7** were transferred from the Schlenk tubes under N$_2$ to a Petri dish and immediately covered with a layer of hydrocarbon oil.[11] Single crystals were selected, mounted on a glass fiber, and immediately placed in a low-temperature N$_2$ stream. Some details of the data collection and refinement are given in Table I. Further details are provided in the supplementary material. All structures were solved by direct methods. Hydrogen attached to nitrogen atoms in structures **5–7** were located in corresponding difference maps and allowed to refine with free positional parameters. The rest of the hydrogen atoms were included at calculated positions by using a riding model with C–H of 0.96 Å and $U_{iso}(H) = 1.2U^*_{iso}(C)$, where U^*_{iso} is the equivalent isotropic thermal parameter (structures **1**, **4** and **5**), or $U_{iso}(H) = 0.04$ Å^2 (structures **6** and **7**). All non-hydrogen atoms were refined anisotropically except in the case of structure **3**, where only P(1) and P(2) were made anisotropic because of a low data/variable ratio. Absorption corrections were applied in the refinements of **1**, **4**, and **6** by the use of the program XABS.[12] Important atom coordinates and isotropic thermal parameters are given in Table II. Important bond distances and angles are listed in Table III.

---

(9) Pestana, D. C.; Power, P. P. *J. Am. Chem. Soc.* **1989**, *111*, 6887.

(10) *International Tables for X-Ray Crystallography*; Kynoch Press: Birmingham, England, 1974; Vol. IV.

(11) This method is described by: Hope, H. *ACS Symp. Ser.* **1987**, *357*, Chapter 10.

(12) Hope, H.; Moezzi, B. Program XABS. University of California, Davis. The program obtains an absorption tensor from F$_o$-F$_c$ differences. See: Moezzi, B. Ph.D. Dissertation, University of California, Davis, 1987.

Table II. Atomic Coordinates ($\times 10^4$) and Isotropic Thermal Parameters ($Å^2 \times 10^3$) for the Important Atoms in Structures **1** and **4**–**7**

	x	y	z	U^a
		Compound **1**		
P(1)	3035 (2)	−68 (1)	2427 (1)	11 (1)
P(2)	1256 (2)	503 (1)	2241 (1)	11 (1)
B	1289 (7)	1417 (3)	2248 (4)	11 (2)
C(1)	4369 (6)	488 (3)	2896 (4)	12 (2)
C(7)	3252 (6)	−252 (3)	1350 (4)	13 (2)
C(13)	193 (5)	−30 (3)	2744 (4)	9 (2)
C(23)	275 (6)	1815 (3)	2653 (4)	10 (2)
C(32)	2230 (6)	1773 (3)	1749 (4)	10 (2)
		Compound **4**		
P	4804 (2)	5674 (1)	4796 (2)	25 (1)
I	2310 (1)	5782 (1)	5428 (1)	34 (1)
C(1)	6902 (6)	6054 (3)	6618 (6)	23 (2)
		Compound **5**		
N(1)	3594 (2)	3227 (2)	5057 (1)	22 (1)
N(2)	4032 (2)	4419 (2)	5117 (1)	24 (1)
H	4209 (19)	4590 (23)	4655 (16)	39 (8)
B(1)	2673 (2)	2965 (3)	4436 (2)	22 (1)
C(1)	2176 (2)	3997 (2)	3778 (2)	20 (1)
C(10)	2149 (2)	1681 (2)	4408 (2)	22 (1)
C(19)	4217 (2)	2415 (2)	5675 (2)	23 (1)
C(25)	3529 (2)	5406 (2)	5329 (2)	23 (1)
		Compound **6**		
N(1)	4604 (1)	834 (1)	7622 (1)	33 (1)
H	4702 (15)	722 (17)	8199 (17)	40
B(1)	3785 (2)	1055 (2)	7069 (2)	33 (1)
C(1)	3734 (1)	1226 (2)	6047 (1)	32 (1)
C(10)	3012 (1)	1135 (2)	7530 (1)	33 (1)
		Compound **7**		
N(1)	−377 (2)	4018 (2)	2249 (2)	43 (1)
H	−560 (20)	4925 (68)	2650 (51)	40
C(1)	−793 (2)	3253 (5)	514 (5)	34 (1)

[a] Equivalent isotropic U defined as one-third of the trace of the orthogonalized U_{ij} tensor.

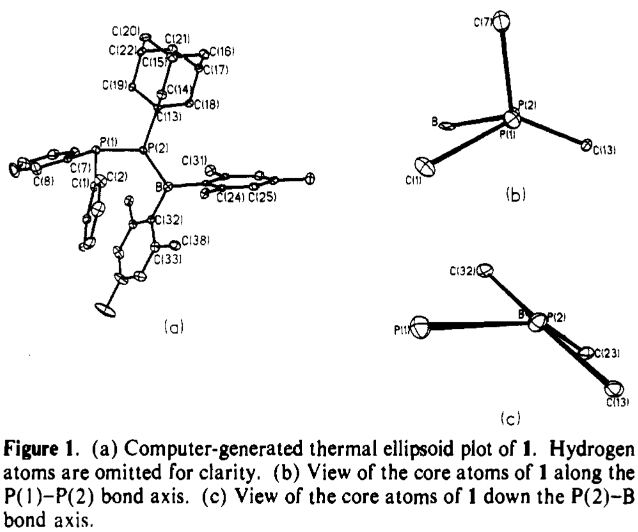

Figure 1. (a) Computer-generated thermal ellipsoid plot of **1**. Hydrogen atoms are omitted for clarity. (b) View of the core atoms of **1** along the P(1)–P(2) bond axis. (c) View of the core atoms of **1** down the P(2)–B bond axis.

Results and Discussion

Structural Descriptions. (a) $Mes_2B(1\text{-}Ad)PPPh_2$ (1). The structure of **1**, which is illustrated in Figure 1a, consists of well-separated molecules of $Mes_2B(1\text{-}Ad)PPPh_2$ that have no imposed symmetry restrictions. The P(1)–P(2) bond is 2.173 (2) Å long, and each of the phosphorus centers has a different geometry. The P(1) atom has pyramidal coordination, and the sum of the angles at P(1) is 317.7°. The P(1)–C(1) and P(1)–C(7) bond lengths are 1.828 (6) and 1.831 (7) Å, respectively. The coordination at P(2) is much closer to planarity, the sum of the angles at P(2) is 350.0 °, and the P(2) atom lies 0.36 Å above the P(1)C(13)B plane. The lengths of the B–P(2) and the P(2)–C(13) bonds are 1.858 (7) and 1.875 (7) Å, respectively. A view of the molecule along the P(1)–P(2) axis is presented in Figure 1b. The angle between the planes containing the bisectors of the C(1)–P(1)–C(7) and B–P(2)–C(13) angles is 68.4°. The boron center has planar coordination, with angles that are close (within 2.4°) to uniform trigonal values. The B–C(23) and B–C(32) bond lengths are 1.598 (10) and 1.591 (10) Å. The angles between the BC_2P plane and the planes of the C(23) and C(32) mesityl rings are 66.9 and 65.0°. When viewed down the P(2)–B axis, the angle between the perpendicular to the plane C(23)B-P(2)C(32) and the bisector of the P(1)–P(2)–C(13) angle is 19.2°, as illustrated in Figure 1c.

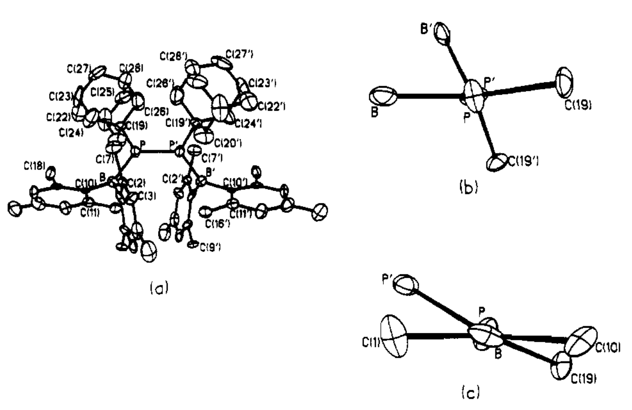

Figure 2. (a) Computer-generated thermal ellipsoid plot of **2**. Hydrogen atoms are omitted for clarity. (b) View of the core atoms of **2** along the P–P′ bond axis. (c) View of the core atoms of **2** along the B–P bond axis.

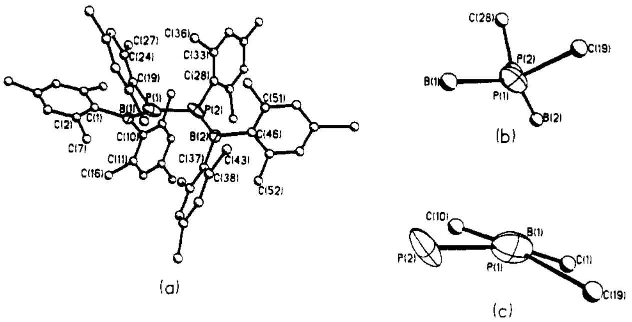

Figure 3. (a) Computer-generated thermal ellipsoid plot of **3**. Hydrogen atoms are omitted for clarity. (b) View of the core atoms of **3** along the P(1)–P(2) bond axis. (c) View of the core atoms of **3** along the P(1)–B(1) bond axis.

(b) $[Mes_2B(1\text{-}Ad)P]_2$ (2). The structure of **2** is illustrated in Figure 2a. It has been described briefly in a preliminary note.[9] It consists of well-separated molecules of $[Mes_2B(1\text{-}Ad)P]_2$ that possess a 2-fold rotation axis through the center of P–P′ bond, which has a length of 2.109 (4) Å. The phosphorus center is almost planar, and P deviates only 0.079 Å from the P′BC(19) plane. The sum of the angles at P is 359.4°, and each angle is very close (within 1.7°) to 120°. A view along the P–P′ bond is presented in Figure 2b; the angles between the bisectors of BPP′C(19) and B′P′PC(19′) planes is 70.9°. The P–C(19) bond is 1.893 (8) Å long. The boron center is planar with angles that have only minor deviations from regularity. The B–C(1) and B–C(10) bond lengths are 1.570 (12) and 1.599 (12) Å, respectively. The angles between C(1) and C(10) mesityl rings and the boron plane are 57.2 and 65.9°. The B–P bond length is 1.852 (9) Å. A view along the B–P axis is shown in Figure 2c. The angle between the perpendicular to the plane C(1)BPC(10) and the bisector of the angle P′–P–C(19) is 25.5°.

(c) $[Mes_2B(Mes)P]_2$ (3). The partially refined structure of **3** is shown in Figure 3a. It also has been described in a preliminary note.[9] The structure consists of discrete molecules of $[Mes_2B(Mes)P]_2$ units that are well separated from each other and have no imposed symmetry restrictions. The coordination of the phosphorus centers is close to planarity, and the sums of the angles at P(1) and at P(2) are 354.9 and 358.6°, respectively. A view

Table III. Important Bond Distances (Å) and Angles (deg) for **1**–**7**

Compound 1			
P(1)–P(2)	2.173 (2)	P(2)–C(13)	1.875 (7)
P(1)–C(1)	1.828 (6)	B–C(23)	1.598 (10)
P(1)–C(7)	1.831 (7)	B–C(32)	1.591 (10)
P(2)–B	1.858 (7)		
C(1)–P(1)–P(2)	106.7 (2)	B–P(2)–C(13)	125.9 (3)
C(7)–P(1)–P(2)	106.0 (2)	C(23)–B–P(2)	119.7 (5)
C(1)–P(1)–C(7)	105.0 (3)	C(32)–B–P(2)	117.6 (5)
B–P(2)–P(1)	121.2 (2)	C(23)–B–C(32)	122.3 (5)
C(13)–P(2)–P(1)	102.9 (2)		
Compound 2			
P–P′	2.109 (4)	B–C(1)	1.570 (12)
P–B	1.852 (9)	B–C(10)	1.599 (12)
P–C(19)	1.893 (8)		
P′–P–B	118.3 (3)	P–B–C(1)	119.3 (7)
P′–P–C(19)	120.6 (3)	P–B–C(10)	118.3 (6)
C(19)–P–B	120.5 (4)	C(1)–B–C(10)	122.3 (7)
Compound 3			
P(1)–P(2)	2.11 (2)	P–C (av)	1.85 (3)
P–B (av)	1.86 (3)	B–C (av)	1.61 (3)
B–P–P (av)	118.0 (2)	B–P–C (av)	122.4 (2)
C–P–P (av)	118.3 (1)		
Compound 4			
P–P′	2.228 (2)	P–C(1)	1.830 (4)
P–I	2.472 (2)		
P′–P–C(1)	96.0 (1)	I–P–C(1)	107.9 (2)
P′–P–C(1)	100.9 (2)		
Compound 5			
N(1)–N(2)	1.439 (3)	N(2)–C(25)	1.407 (4)
N(1)–B(1)	1.419 (3)	B(1)–C(1)	1.582 (4)
N(1)–C(19)	1.439 (3)	B(1)–C(10)	1.587 (4)
N(2)–H	0.911 (30)		
N(2)–N(1)–B(1)	120.9 (2)	C(25)–N(2)–N(1)	118.1 (2)
C(19)–N(1)–B(1)	128.0 (2)	N(1)–B(1)–C(1)	118.0 (2)
C(19)–N(1)–N(2)	111.0 (2)	N(1)–B(1)–C(10)	121.1 (2)
N(1)–N(2)–H	111.1 (16)	C(1)–B(1)–C(10)	120.9 (2)
C(25)–N(2)–H	111.3 (17)		
Compound 6			
N(1)–N(1)′	1.411 (4)	B(1)–C(1)	1.597 (3)
N(1)–B(1)	1.384 (3)	B(1)–C(10)	1.588 (4)
N(1)–H	0.877 (26)		
B(1)–N(1)–N(1)′	125.9 (2)	C(1)–B(1)–N(1)	116.1 (2)
H–N(1)–N(1)′	110.6 (15)	C(10)–B(1)–N(1)	116.2 (2)
B(1)–N(1)–H	123.3 (16)	C(1)–B(1)–C(10)	127.7 (2)
Compound 7			
N(1)–N(1)′	1.394 (7)	N(1)–H(1)	0.861 (47)
N(1)–C(1)	1.386 (4)		
N(1′)–N(1)–C(1)	118.1 (4)	C(1)–N(1)–H(1)	117.4 (21)
N(1′)–N(1)–H(1)	116.2 (25)		

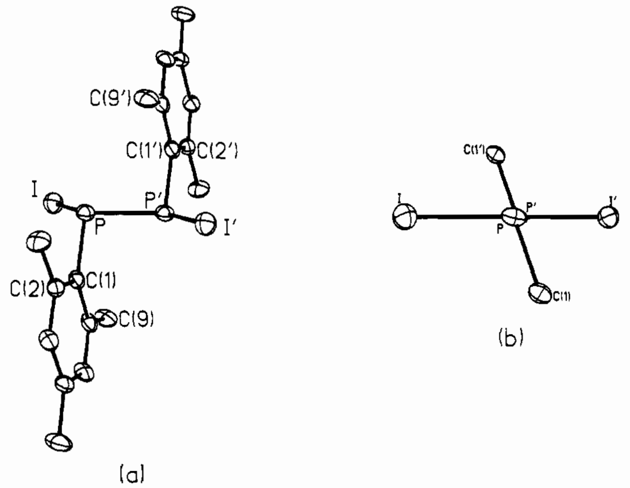

Figure 4. (a) Computer-generated thermal ellipsoid plot of **4**. Hydrogen atoms are omitted for clarity. (b) View of the core atoms of **4** along the P–P′ bond axis.

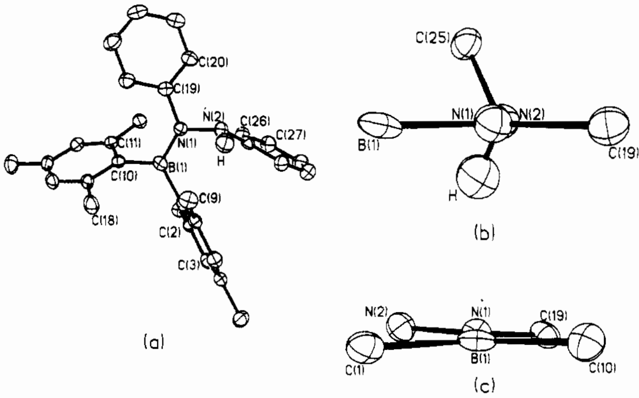

Figure 5. (a) Computer-generated thermal ellipsoid plot of **5**. Hydrogen atoms on the phenyl and mesityl rings are omitted for clarity. (b) View of the core of **5** along the N(1)–N(2) bond axis. (c) View of the core atoms of **5** along the N(1)–B(1) bond axis.

down the P(1)–P(2) axis shows that the angle between the bisectors of the angles B(1)–P(1)–C(19) and B(2)–P(2)–C(28) is 83.5° (Figure 3b). The P(1)–P(2) bond is 2.11 (2) Å long. The average B–P distance is 1.86 (3) Å. The average P–C bond length is 1.85 (3) Å. The C(19) and C(28) mesityl rings are at angles of 68.4 and 68.9° with respect to the phosphorus planes. The B centers are planar with angles deviating from regular trigonal values by ~5°. A view along the P(1)–B(1) axis is shown in Figure 3c; the average angle between perpendicular to the plane CBPC and the bisector of the P–P–C angle is 6.4°. The B–C bonds average 1.85 (3) Å in length. The angles between the C(1) and C(10) mesityl rings and the B(1)C(1)C(10) plane are 57.5 and 67.9°, respectively. The angles between the B(2)C(37)C(48) plane and the C(37) and C(46) ring planes are 59.5 and 62.5°.

(d) [Mes(I)P]$_2$ (4). The structure of **4** is presented in Figure 4a. It consists of well-separated molecules of [Mes(I)P]$_2$, which have an inversion center through the center of the P–P′ bond. The coordination at P is pyramidal, and the sum of the angles at P is 304.8°. The P–P′ bond distance is 2.228 (2) Å, and the P–I and P–C(1) bond lengths are 2.472 (2) and 1.830 (4) Å. The angle between the perpendicular to the C(1) ring and the bisector of the angle I–P–P′ viewed down the P–C(1) axis (Figure 4b) is 77.6°.

(e) Mes$_2$B(Ph)NN(Ph)H (5). The structure of **5** is illustrated in Figure 5a and consists of well-separated molecules of Mes$_2$B(Ph)NN(Ph)H that have no imposed symmetry restrictions. The nitrogen centers differ in their geometrical features. The N(1) center is planar, with irregular angles in the range 111–128°. The N(1)–C(19) bond is 1.439 (3) Å long, and the dihedral angle for the C(19) phenyl ring is 36.9°. The B–N(1) distance is 1.419 (3) Å. The N(2) center has a pyramidal configuration with the sum of the angles equal to 340.5°. The N(2)–C(25) bond length is 1.407 (4) Å. A view down the N(1)–N(2) bond, which is 1.439 (3) Å long, is shown in Figure 5b. The angle between the perpendicular to B(1)N(1)N(2)C(19) plane and the bisector of the C(25)–N(2)–H angle is 88.7°. The boron center is planar, with angles that are all within 2.0° of 120°. The B(1)–C(1) and B(1)–C(10) bonds are 1.582 (4) and 1.587 (4) Å long. The angles between the C(1) and C(10) mesityl ring planes and the plane containing B(1) are 62.9 and 62.2°, respectively. The twist angle between the N(1) and B(1) planes is 4.7° (Figure 5c).

(f) [Mes$_2$B(H)N]$_2$ (6). The structure of **6** is illustrated in Figure 6a. It consists of discrete molecules of [Mes$_2$B(H)N]$_2$ that have a 2-fold rotation axis through the center of the N(1)–N(1′) bond, which is 1.411 (4) Å long. The sum of the angles at the N(1) center is 359.8°, although they display considerable deviation from regularity (Table III). A view along the N(1)–N(1′) axis shows that the twist angle between the N(1) and N(1′) planes is 25.9°

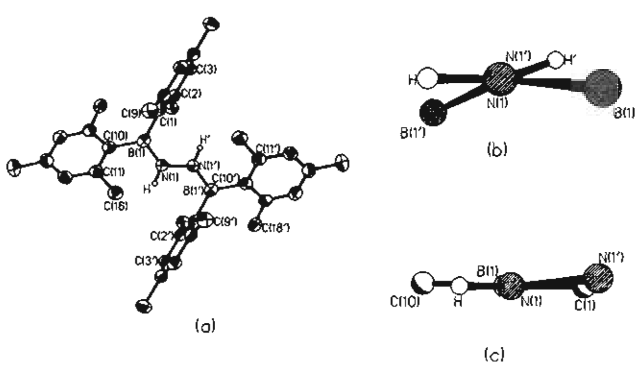

Figure 6. (a) Computer-generated thermal ellipsoid plot of **6**. Hydrogen atoms on the mesityl rings are omitted for clarity. (b) View of the core atoms of **6** along the N(1)–N(1′) bond axis. (c) View of the core atoms of **6** along the N(1)–B(1) bond axis.

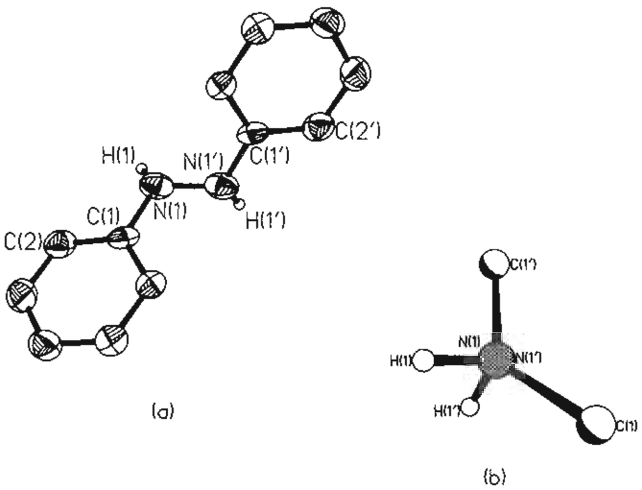

Figure 7. (a) Computer-generated thermal ellipsoid plot of **7**. Hydrogen atoms on the phenyl rings are omitted for clarity. (b) View of the core atoms of **7** along the N(1)–N(1′) bond axis.

(Figure 6b). The B(1) center is planar, and the B(1)–N(1) bond is 1.384 (3) Å long. The twist angle between the N(1) and B(1) planes is 3.9°, as shown by the view along the N(1)–B(1) axis in Figure 6c. The B(1)–C(1) and B(1)–C(10) bond lengths are 1.597 (3) and 1.588 (4) Å. The C(1) and C(10) mesityl rings reside at angles of 72.8 and 51.1° with respect to the boron plane.

(g) $[Ph(H)N]_2$ (7). The structure of **7** is shown in Figure 7a. It consists of discrete molecules of $[Ph(H)N]_2$ that possess a 2-fold rotation axis through the center of the N(1)–N(1′) bond, which is 1.394 (7) Å in length. The nitrogen center is pyramidal although the sum of the angles at N(1) is 351.7°, and the N(1) atom is only 0.19 Å above the H(1)C(1)N(1′) plane. The view along the N(1)–N(1′) bond is presented in Figure 7b. The angle between the bisectors of the H(1)–N(1)–C(1) and C(1′)–N(1′)–H(1′) angles is 87.0°. The N(1)–C(1) bond length is 1.386 (4) Å; a view down the N(1)–C(1) axis shows that the angle between the perpendicular to the C(1) phenyl ring and the bisector of H(1)–N(1)–N(1′) angle is 1.9°.

Discussion

The Boryldiphosphanes 1–3 and the Diphosphane 4. Compounds **1–3** are the first boryl-substituted diphosphanes to be characterized by X-ray diffraction and ^{1}H, ^{31}P, and ^{11}B NMR spectroscopy. Species **1** was prepared by a straightforward synthesis that involved the in situ preparation of the borylphosphide compound $Mes_2BP(1\text{-}Ad)Li(Et_2O)_2$, followed by a salt elimination reaction with Ph_2PCl to afford **1** in moderate yield as indicated by the equation

$$Mes_2BP(1\text{-}Ad)Li(Et_2O)_2 + ClPPh_2 \xrightarrow{Et_2O} LiCl + \underset{\mathbf{1}}{Mes_2B(1\text{-}Ad)PPPh_2}$$

Compounds **2** and **3** were prepared from the corresponding lithium borylphosphide salts via their reaction with a transition-metal halide such as $CrCl_3$ as indicated by the equation

$$Mes_2B(R)PLi(Et_2O)_3 + CrCl_3 \xrightarrow{THF} CrCl_2 + LiCl + \tfrac{1}{2}\underset{\mathbf{2,\ 3}}{[Mes_2B(R)P]_2}$$

The reaction apparently results in the oxidation of the $[PRBMes_2]^-$ anion (R = 1-Ad (**2**), Mes (**3**)) to the radical $[PRBMes_2]^\bullet$. The latter probably rapidly dimerizes to give either **2** or **3**. The concomitant formation of $CrCl_2 \cdot 2THF$ was also observed. The crystalline purple flakes of $CrCl_3$ gradually transformed into a green-gray powder during the course of the reaction. Attempts to prepare $Mes_2BPMesI$ from the reaction of $Mes_2BPMesLi(Et_2O)_2$ with I_2 resulted in the isolation of crystals of $[Mes(I)P]_2$ (**4**) instead. Even though care was taken to add I_2 to the $Mes_2BPMesLi(Et_2O)_2$ solution very slowly, the reaction seems to proceed according to the equation

$$2Mes_2BPMesLi(Et_2O)_2 + 3I_2 \rightarrow \underset{\mathbf{4}}{[Mes(I)P]_2} + 2LiI + 2Mes_2BI$$

In support of this reaction stoichiometry, the ^{31}P NMR spectrum of the crude product showed a signal at $\delta = 60$, corresponding to some unconsumed $Mes_2BPMesLi(Et_2O)_2$ starting material. The structure of **4** is similar to previously reported diphosphane structures.[5] The P–P′ bond length of 2.228 (2) Å is in the normal range as are the angles at P ($\sum°P = 304.8°$), which are considerably smaller (by as much as 13.0°) than tetrahedral values, indicating that the phosphorus bonding orbitals have considerably reduced s character. There is a crystallographic imposition of an anti conformation (inversion center through the P–P bond) on the molecule. This is in accord with the preference found in tetraaryldisilenes and -diphosphanes to adopt anti configuration as the bulkiness of aryl groups increases.[13]

The structures of **1–3** are in sharp constrast to all the published diphosphane structures.[5,13] Their most conspicuous feature is the planarity (or near planarity) of the boryl-substituted phosphorus centers. In addition, the P–P bonds (~2.11 Å) in **2** and **3** are shorter than any previously known unconstrained single P–P bond lengths. The "mixed" diphosphane, **1**, has a P–P bond length (2.173 (2) Å) that falls between the P–P distances in **2** or **3** and those found in normal diphosphanes. The P–P bond lengths in **2** and **3** are approximately halfway between the values for normal single[5] and double P–P bonds[1c,4] (2.22 and 2.02 Å). Short P–P distances of 2.129, 2.147 (1), and 2.118 Å have been observed in highly strained cage compounds that contain a P–P moiety.[14] Calculations have accounted for this phenomenon in terms of olefinic character.[15] In the case of **1–3**, however, the experimental evidence points to an explanation of the shortened P–P bonds that is primarily based on a changed hybridization at the phosphorus atoms. The reasons for this conclusion are now discussed in more detail.

First, the planarity of the boryl-substituted phosphorus centers in **1–3** may be compared to some recently reported monomeric organophosphinoboranes that have displayed planar boron and phosphorus centers with coordination at B and P that is very close to planarity.[16] These compounds also displayed small twist angles (<10°) between the planes at B and P. Thus, the B–P bonding was interpreted on the basis of sp^2 hybridization at the boron and

---

(13) Baxter, S. G.; Cowley, A. H.; Davis, R. E.; Riley, P. E. *J. Am. Chem. Soc.* **1981**, *103*, 1699–1702 and references therein.

(14) Niecke, E.; Rüger, R.; Krebs, A. *Angew. Chem., Int. Ed. Engl.* **1982**, *21*, 544. Binger, P.; Biedenbach, B.; Krüger, C.; Regitz, M. *Angew. Chem., Int. Ed. Engl.* **1987**, *26*, 764. Barron, A. R.; Cowley, A. H.; Hall, S. W.; Nunn, C. M. *Angew. Chem., Int. Ed. Engl.* **1988**, *27*, 837.

(15) Schoeller, N. W.; Staemmler, V.; Rademacher, P.; Niecke, E. *Inorg. Chem.* **1984**, *25*, 4382.

(16) For a review on phosphinoborane compounds having B–P bonds with multiple character see: Power, P. P. *Angew. Chem., Int. Ed. Engl.* **1990**, *29*, 449.

phosphorus atoms and the presence of a π-interaction between the P lone pair and the empty B p orbital.[16] The B–P bonding in **1**–**3** can be interpreted similarly. Thus, the B–P bond geometries **1**–**3** support σ-bonding between sp^2-hybridized B and P centers and, in addition, a significant degree of multiple bonding from the overlap of B and P orbitals. The shortness of the B–P bonds in **1**–**3** is underlined by the fact that they are not as long as the P–C bonds in the same molecule even though boron has a radius that is larger (by about 0.06 Å) than that of carbon. The twist angles between the boron and phosphorus "planes" in structures **1** and **2** are somewhat larger (19.2 and 25.5°, respectively) than those observed in **3** or in the previously reported lithium borylphosphide salts.[17,18] The increased twist angles can be traced to the large steric requirements of both the boryl and phosphorus substituents. The boryl-substituted P(2) center in compound **1** has the greatest deviation from planarity, with angles that total 350.0°. In addition, the ^{11}B chemical shift observed in **1** (δ = 72.3) is further downfield (~20 ppm) than the shifts in **2** or **3**. This is in harmony with the somewhat nonplanar character of the phosphorus in **1**, which suggests that the lone-pair delocalization onto boron is not as efficient in this compound as it is in **2** or **3**. Nonetheless, the P(2) atom is only 0.36 Å out of the plane formed by the atoms P(1), C(13), and B. These angles may be contrasted with the angular sum of 317.7° found at P(1) in the same structure or with 304.8° found at P in compound **4**.

The large twist angles (70.9 and 83.5°) between the P–P′ and P(1)–P(2) planes in structures **2** and **3** do not support any significant butadiene-like interaction between the two BP moieties that might account for a shortened P–P bond in terms of extended bonding between the four p orbitals of the BPPB array. The lack of multiple P–P interaction in **2** and **3** is also supported by the ^{31}P NMR data. The ^{31}P NMR chemical shifts for compounds with multiple P–P bonds are usually observed several hundred ppm downfield[3a,4] whereas the shifts observed for **1**–**3** appear in the range −25 to 25 ppm, where many diphosphanes are normally observed.[19] Compound **1** represents an intermediate case between the 1,2-diboryldiphosphanes **2** and **3** and normal disphosphanes like **4**. The two phosphorus centers, one almost planar and one pyramidal, are clearly distinguished by ^{31}P NMR data, and the P–P coupling constant is 316.5 Hz, although its sign has not yet been determined. The P(1)–P(2) bond length of 2.173 (2) Å agrees well with the interpolated value of 2.16 Å. Furthermore, preliminary calculations on the hypothetical $[H_2B(H)P]_2$ molecule[20] indicate that its lowest energy configuration features nonplanar phosphorus atoms with a P–P distance of 2.17 Å, whereas if the phosphorus atoms have planar coordination, the P–P bond is 2.12 Å long, in good agreement with the experimental findings described.

A further consideration in the discussion of the short P–P bond lengths is the possible role played by reduced lone-pair–lone-pair repulsion between the phosphorus centers. In **1** and, in particular, **2** and **3** the lone pairs are engaged in π-bonding with boron p orbitals. The reduced interelectronic repulsion resulting from the removal of electron density onto B could account for some of the observed shortening. However, calculations[23] and experimental data[4] on *cis*- and *trans*-diphosphenes give almost identical P–P distances although the relative distance between the lone pairs changes significantly. This suggests that this factor probably has only a minor effect on the P–P bond length.

Scheme I. Attempts To Prepare $[Mes_2B(Ph)N]_2$

$$\text{a) } \mathbf{5} + \text{n-BuLi} \xrightarrow[\text{3 h}]{\text{THF ref.}} \text{dk-yellow sol.} \xrightarrow[\text{reflux 12 h}]{Mes_2BF} \text{white precipitate} \longrightarrow Mes_2BOH \text{ crystals isolated}$$

$$\text{b) } [Ph(H)N]_2 + 2\,Mes_2BF + 2Et_3N(\text{excess}) \xrightarrow[\text{14 h}]{\text{hexane reflux}} [Mes_2B(OH)_2]^- [NHEt_3]^+ \text{ crystals}$$

$$\text{c) } 2Mes_2BN(Ph)H + Pb(Ac)_4 \xrightarrow{C_6H_6} \text{no reaction}$$

In sum, the above evidence suggests that the contraction in the P–P bond distances in **1**–**3** is primarily a result of changes in the hybridization of the phosphorus σ-bonding orbitals. The variation of P–P distances with the hybridization or coordination number at the phosphorus centers has adequate precedent in the study of four- and five-coordinate phosphorus species.[21,22] These compounds, however, did not exhibit the dramatic changes in P–P bond lengths seen in **2** or **3**. The amount of the shortening observed in **2** and **3** suggests that about half of the difference in length between a double and a single P–P bond is due to the rehybridization and the remainder is attributable to π-overlap of the p orbitals. This conclusion is also borne out by the recent calculations on the hypothetical species *trans*-HPPH.[23] These have shown that the bonding π orbital in this species (which is the HOMO) appears at an energy of 7.69 eV below the LUMO whereas the stabilization of the σ(PP) bond is 25.02 eV. In addition, estimates of the rotational barrier in diphosphenes vary from 20 to 35 kcal mol^{-1},[4,23,24a] whereas the strength of π-bonds in alkenes is 50–60 kcal mol^{-1}.[24b] These figures are in good agreement with the respective proportions of contraction due to p–p π-overlap. Other support comes from calculations[24c] on the hypothetical diphosphene transition-metal complex $H_2P_2Cr(CO)_5$ that indicate a large amount (0.3 electron) of back-donation by the metal fragment into the b_g (π*-type) orbital of the ligand. However, this extensive transfer of electron density into the ligand antibonding orbital results in only slight lengthening of the P–P bond upon complexation. This result, which is in agreement with structural and spectroscopic studies, is consistent with weaker p–p orbital interactions.

The Borylhydrazines 5–7. Although boryl derivatives of hydrazines have been known for a long time[25,26] relatively few had been structurally characterized. The structures of two borylhydrazine moieties as part of ring systems have been determined. These are the compounds $[-B(NMe_2)N(Me)(Me)N-]_2$ (**8**)[27] and the 1,2-hydrazinediylidenetetrakis(boranediyl) disulfide **9**.[28] They have N–N distances of 1.431 (2) Å for **8** and 1.449 (2) Å for **9**. These distances are marginally shorter than the 1.46 Å observed in hydrazine[29] or 1.45 Å in *N,N′*-dimethylhydrazine.[30] In addition,

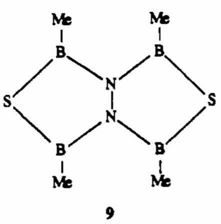

9

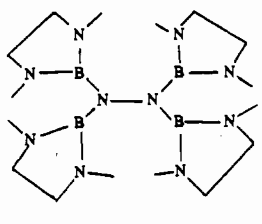

10

---

(17) Bartlett, R. A.; Feng, X.; Power, P. P. *J. Am. Chem. Soc.* **1986**, *108*, 5007.

(18) Bartlett, R. A.; Dias, H. V. R.; Feng, X.; Power, P. P. *J. Am. Chem. Soc.* **1989**, *111*, 1306.

(19) Mark, V.; Duncan, C. H.; Crutchfield, M. M.; van Wager, J. R. In *Topics in Phosphorus Chemistry*; Grayson, M., Griffith, E. J., Eds.; Wiley: New York, 1967; Vol. 5, Chapter 4.

(20) These results are based upon STO-3G calculations. Calculations at a more sophisticated level are currently in progress: Fink, W. H. Unpublished work.

(21) Schomburg, D.; Weferling, N.; Schmutzler, R. *J. Chem. Soc., Chem. Commun.* **1981**, 609.

(22) Schomburg, D.; Betterman, G.; Ernst, L.; Schmutzler, R. *Angew. Chem.* **1985**, *97*, 971.

(23) Allen, T. L.; Scheiner, A. C.; Yamaguchi, Y.; Schaefer, H. F. *J. Am. Chem. Soc.* **1986**, *108*, 7579.

(24) (a) Cominade, A.-M.; Verrier, M.; Ades, C.; Paillons, N.; Koenig, M. *J. Chem. Soc., Chem. Commun.* **1984**, 875. (b) Miller, S. I. *J. Chem. Educ.* **1978**, *55*, 778. (c) Schugart, K. A.; Fenske, R. F. *J. Am. Chem. Soc.* **1985**, *107*, 3384.

(25) 1,2-Diborylhydrazine, $[H_2B(H)N]_2$, was first synthesized by: Goubeau, J.; Ricker, E. *Z. Anorg. Allg. Chem.* **1961**, *310*, 123. Niedenzu, K.; Dawson, J. W. *Boron-Nitrogen Compounds*; Springer-Verlag: Berlin, 1965.

(26) Nöth, H.; Regnet, W. *Adv. Chem. Ser.* **1964**, *42*, 166–182.

(27) Huffman, J. C.; Fusstetter, H.; Nöth, H. *Z. Naturforsch.* **1976**, *31B*, 289.

(28) Nöth, H.; Ullmann, R. *Chem. Ber.* **1975**, *108*, 3125.

Scheme II. Attempts To Prepare $[(Mes_2B)_2N]_2$

$$\text{a)}\quad 6 + 2n\text{-BuLi} \xrightarrow[2\text{ h}]{\text{reflux THF}} \text{yellow solution} \xrightarrow[\text{reflux 10 h}]{Mes_2BF} \text{starting material } 6$$

$$\text{b)}\quad 6 + 2Mes_2BF + 2NEt_3(\text{excess}) \xrightarrow{\text{hexane}} \text{white precipitate} \xrightarrow{\text{reflux 10 h}} \text{starting material } 6$$

the structure of the tetraborylhydrazine **10** has been determined.[31] In this case, each boryl group is also substituted by amine ligands, which may compromise the π-interaction between the boron and the hydrazine nitrogens. The N–N distance in this case is 1.464 (10) Å. In order to gauge the effect of boryl substitution and to draw comparisons between the hydrazine and diphosphanes, it was decided to synthesize several novel acyclic alkyl- or aryl-substituted borylhydrazines. The compounds **5** and **6** are the first (diarylboryl)hydrazines to be characterized by X-ray diffraction and ^1H and ^{11}B NMR spectroscopy. Treatment of 1,2-diphenylhydrazine with 2 equiv of *n*-BuLi, followed by the reaction with 2 equiv of Mes_2BF, gave **5** in moderate yield. Although the

$$[Ph(H)N]_2 + 2n\text{-BuLi} \xrightarrow[\text{THF, reflux}]{2Mes_2BF} \underset{\mathbf{5}}{Mes_2B(Ph)NN(Ph)H} + 2LiF + Mes_2B(n\text{-Bu})$$

dilithiation of 1,2-diphenylhydrazine has been reported previously,[26,32] **5** was the only product isolated when this reaction was repreated by refluxing for 12 h in THF. Other attempts to isolate the 1,2-diboryl-1,2-diphenylhydrazine $[Mes_2B(Ph)N]_2$ are illustrated in Scheme I. The failure of these routes is probably due to the large size of the substituents on B and N. The synthesis of **6** was accomplished by the standard method[26] of refluxing the hydrazine with the halogenodiorganoborane in a hydrocarbon solvent, where the HF byproduct was trapped as triethylammonium fluoride as shown in the equation

$$NH_2NH_2 + 2Mes_2BF + NEt_3\ (\text{excess}) \rightarrow \underset{\mathbf{6}}{[Mes_2B(H)N]_2} + [NHEt_3]^+[F]^-$$

The exclusive isolation of **6** instead of the 1,1-disubstituted isomer is also attributable to steric hindrance. This work is in agreement with previous studies on the synthesis of diborylhydrazines in which only the 1,2-isomers were obtained.[26] Further attempts to isolate $[(Mes_2B)_2N]_2$ are described in Scheme II.

The primary structural features of **5** and **6** are the planar coordination of the nitrogen atoms bonded to the Mes_2B– group and the shortened N–N bond distances. These features are in contrast to those found in hydrazine[29] and in 1,1- and 1,2-dimethylhydrazine,[30] where the N–N distances are 1.46 (2) and 1.45 (3) Å, respectively, and the N centers have pyramidal coordination. The B–N bonds in **5** and **6** are in the range found for the aminoboranes $R_2BNR'_2$ and are indicative of multiple B–N bonding.[33] The low dihedral angles (<10°) between the B and N planes in **5** and **6** are also in harmony with a multiple B–N interaction.[33] The large deviations of the angles from the regular trigonal value of 120° at the nitrogen atoms in compounds **5** (111–128°) and **6** (111–125°) are also found in the related aminoborane $Mes_2BN(Ph)H$ (112–130.6°).[34] These asymmetries are probably due to the larger steric requirements and different bonding characteristics of the Mes_2B–substituent in comparison to H or Ph.

Table IV. Comparison of the N–N Bond Lengths and Twist Angles in Selected Hydrazine Derivatives

compd	N–N bond, Å	N–N twist angle,[a] deg	ref
$Mes_2B(Ph)NN(H)Ph$ (**5**)	1.439 (3)	88.7	this work
$Mes_2B(H)NN(H)BMes_2$ (**6**)	1.411 (4)	25.9	this work
$[Ph(H)N]_2$ (**7**)	1.394 (7)	87.0	this work
$[B(NMe_2)N(Me)N(Me)]_2$ (**8**)	1.431 (2)	19.3	27
9	1.449 (2)	18.0	28
10	1.446 (10)	56.6	31
$[H(O)C(H)N]_2$ (**11**)	1.392 (7)	0	35
$[Ph_2N]_2$ (**12**)	1.406 (4)	74.1	37

[a] Defined as the angle between the perpendiculars to the N planes when viewed down the N–N bond axis.

The N–N bonds in **5** and **6** may be compared with the values in **8**–**10** (Table IV) and also with the N–N bond distance 1.392 (7) Å in diformylhydrazine (**11**).[35] The latter species features a planar array of non-hydrogen atoms. Compounds **5**–**12**, therefore, mostly feature bonding between planar or nearly planar nitrogen atoms. The longer N–N bonds in **8** (in which boron is also substituted by an NMe_2 group and two hydrazine nitrogens), in **9** (in which the N atoms are substituted by two boryl substituents), and in **10** can be attributed to competitive factors not present in **5**–**7** and in **11** and **12**. The lengthening of the N–N bond (1.439 (3) Å) in **5** can be attributed to the nonplanarity and changed hybridization at N(2) ($\sum°N = 340.5°$). All the remaining N–N bonds are nearly 1.4 Å long. In sum, these data appear to indicate that the normal N–N distance between two planar nitrogen centers is in the range 1.39–1.41 Å. The distance is about 0.05 Å shorter than the N–N bond length (1.45 Å) that is observed when pyramidal nitrogens are present as in hydrazine[29] and 1,2-dimethylhydrazine.[30] It is notable, however, that 1.39–1.41 Å bond length is much longer than the 1.25 Å normally observed for N–N double bonds.[35,36] In effect, only about a quarter of the bond contraction observed in the N–N case may be attributed to a rehybridization. The remainder is due to the p–p π-overlap. This view of the bonding is also in good agrement with structural data for C–N compounds that involve a variety of different hybridizations at carbon and nitrogen.[6,32]

It is, of course, also possible to make an analogy between butadiene and compound **6**. However, comparison of the twist angles between the N planes in **6** (25.9°, N–N = 1.411 (4) Å) and in tetraphenylhydrazine, Ph_2NNPh_2 (74.1°, N–N = 1.406 (4) Å)[37] suggests that the N–N bond length is not greatly affected by the magnitude of this angle. Indeed, the slightly shorter distance in Ph_2NNPh_2 suggests a negative correlation. In addition, arguments concerning lone-pair repulsions[32] could be used to account for the longer N–N bonds in hydrazines that are pyramidal at N. No doubt the repulsions probably figure more prominently in the hydrazines than in the diphosphanes. Nonetheless, the reduced lone-pair–lone-pair repulsion rationale for the shortened N–N bond lengths is not strongly supported by a comparison of the data for **5** and **7**. In **5**, the lone pair at the planar N(1) center is involved in bonding with boron and on N(2) the substituents H and Ph are the same as those on both nitrogens in **7**. If, in **5**, it is assumed that the lone pair on N(1) is indeed delocalized onto boron, it follows that the repulsion should be greater in **7** than in **5**. The N–N distance is, however, significantly longer in **5** than it is in **7**, which is contrary to what has been predicted on the basis of lone-pair repulsions. It should also be borne in mind that there is evidence for significant delocalization in diphenylhydrazine (**7**). As already mentioned, its N–N bond

---

(29) Collin, R. L.; Lipscomb, W. N. *Acta Crystallogr.* **1951**, *4*, 10.

(30) Beamer, W. H. *J. Am. Chem. Soc.* **1948**, *70*, 2979.

(31) Bharara, P. C.; Nöth, H. *Z. Naturforsch.* **1978**, *34B*, 1352.

(32) Smith, P. A. S. *Derivatives of Hydrazines and Other Hydronitrogens Having N-N-Bonds*; Benjamin/Cummings: Reading, MA, 1983.

(33) Lappert, M. F.; Power, P. P.; Sanger, A. R.; Srivastava, R. C. *Metal and Metalloid Amides*; Ellis-Horwood: Chichester, U.K., 1980; pp 88–99.

(34) Bartlett, R. A.; Feng, X.; Olmstead, M. M.; Power, P. P.; Weese, K. J. *J. Am. Chem. Soc.* **1987**, *109*, 4851.

(35) Tomie, T.; Koo, C. H.; Nitla, I. *Acta Crystallogr.* **1958**, *11*, 774.

(36) Mostad, A.; Romming, C. H. R. *Acta Chem. Scand.* **1971**, *25*, 3561 and references therein.

(37) Hoekstra, A.; Vos, A.; Braun, P. B.; Hornstra, J. *Acta Crystallogr.* **1975**, *B31*, 1708. Hoekstra, A.; Vos, A. *Acta Crystallogr.* **1975**, *B31*, 1722.

is unexpectedly short. In addition, the N–C distance observed (1.386 (4) Å) is marginally shorter than the N(2)–C(25) bond (1.407 (6) Å) in **5**. Also, the average C–C distance in the phenyl ring in **7** (1.39 Å) is marginally longer than the corresponding distance in **5** (1.38 Å). This supports a stronger interaction between the nitrogen p orbital and an antibonding aromatic π orbital in the case of **7**. Irrespective of which effects (lone-pair–lone-pair repulsion, rehybridization, or delocalization) predominate in the hydrazine derivatives, it is a fact that the range of N–N bond lengths is 1.394 (7)–1.46 Å, which is less than 30% of the difference in length between an N–N single and an N–N double bond.

In summary, the data in this paper show that, in the case of N–N and P–P bonds, σ-orbital rehybridization effects become more important and P–P π-bonding contributions are considerably diminished in the heavier element pairs. Studies of the effects of rehybridization on bond distances in other heavier main-group element derivatives are continuing.

Acknowledgment. We wish to thank the National Science Foundation (Grant CHE-8618739 and Instrumentation Grant CHE-8802721) for supporting this research.

Supplementary Material Available: Tables of atom coordinates, crystallographic data, and a summary of data collection and refinement and full tables of bond distances and angles, hydrogen coordinates, and anisotropic thermal parameters (20 pages); listings of structure factors (61 pages). Ordering information is given on any current masthead page.

Contribution from the H. L. Hunter Chemistry Laboratory,
Clemson University, Clemson, South Carolina 29634-1905

Cesium Fluoride Promoted Halogenation of Cyanogen by Chlorine and Bromine and Selected Reactions of Products[1]

Qui-Chi Mir and Darryl D. DesMarteau*

Received February 1, 1990

The reaction of cyanogen with Cl_2 and Br_2 in the presence of CsF gives rise to a series of compounds, $NCCF{=}NX$ (Cl, Br), $XN{=}CF{-}CF{=}NX$ (Br), and $NCCF_2NX_2$ (Cl). Subsequent reactions of $NCCF_2NCl_2$ with MF/Br_2 (M = Cs, K, Na) give rise to $X'N{=}CFCF{=}NX$, $XN{=}CFCF_2NXX'$, and $NCCF_2NXX'$ (X, X' = Cl, Br), involving oxidation and exchange of Cl by Br. Fourteen compounds were identified by ^{19}F NMR and mass spectrometry, and 10 of the compounds have not been previously reported. Photolysis of $NCCF{=}NX$ and $NCCF_2NXX'$ gives rise to the respective azine and diazene. The azine undergoes a fluoride ion induced cyclization to form a novel cyclic, 4-membered diazo compound. Thermal additions of $NCCF{=}NBr$ with C_2F_4 and $CF_2{=}CCl_2$ produced only traces of the expected adducts. New compounds identified were $NCCF{=}NCl$ (**1**), $NCCF_2NCl_2$ (**2**), $NCCF{=}NBr$ (**4**), $NCCF_2NBrCl$ (**14**), $NCCF_2NBr_2$ (**15**), $NCCF{=}N{-}N{=}CFCN$ (**16**), $NCCF_2N{=}NCF_2CN$ (**17**), and $NC\overline{CFN{=}NC}FCN$ (**18**), and $ClN{=}CFCF{=}NBr$ (**7**), $BrN{=}CFCF_2NCl_2$ (**9**), $BrN{=}CFCF_2NClBr$ (**10**), $ClN{=}CFCF_2NClBr$ (**11**), and $ClN{=}CFCF_2NBr_2$ (**12**), which could only be identified in a mixture. Some evidence for $NCCF{=}NC_2F_4Br$ (**19**) and $NCCF{=}N(CF_2CCl_2)Br$ (**20**) was also found in the addition of **4** to the respective alkenes. Alternative routes to the previously known compounds $BrN{=}CFCF{=}NBr$ (**5**), $ClN{=}CFCF{=}NCl$ (**6**), $Cl_2NCF_2CF_2NCl_2$ (**3**), $ClN{=}CFCF_2NCl_2$ (**8**), and $BrN{=}CFCF_2NBr_2$ (**13**) were also identified.

Introduction

Cesium fluoride has been shown to be an effective reagent for the fluoride-promoted oxidation of $R_fCF{=}NF$ by Cl_2 and Br_2 to form R_fCF_2NFX, of R_fCN to $R_fCF_2NCl_2$ and $R_fCF{=}NBr$,[2,3] of $R_xN{=}CF_2$ to $R_xN(X)CF_3$,[4] of $CF_2{=}NX'$ (X' = F, Cl, Br) to $CF_3NX'X$,[2,5,6] of R_fCN by F_2 to R_fCFNF_2,[7] and of certain hindered imines $R_fN{=}CFR_f'$ by ClF to $R_fNClCF_2R_f'$.[8] These reactions are quite general with fluorinated imines and nitriles and are believed to occur via intermediate anions $R_fCF{=}N^-$, $R_fNX'^-$, and $R_xNCF_3^-$, although in most instances definitive evidence for the proposed anion intermediates is lacking. In an interesting extension of these fluoride-promoted reactions, we examined the reactivity of $N{\equiv}CCF{=}NF$ and found both multiple bonds were oxidized by Br_2 but only the imine function was reactive with Cl_2.[9] This work prompted us to examine the reactions of cyanogen under similar conditions to compare the reactivity of Cl_2 and Br_2 and to see if a selective and stepwise oxidation of the triple bonds was possible.[10] Of the 49 structural isomers possible in $X_2NCF_2CF_2CF_2NX_2$, $XN{=}CFCF{=}NX$, $XN{=}CFCF_2NX_2$, $NCCF_2{=}NX_2$, and $NCCF{=}NX$ for combinations of chlorine bromine and fluorine, at least 24 have now been positively identified.

Experimental Section

General Methods. All work was carried out in a conventional Pyrex vacuum system equipped with glass–Teflon valves. Pressures were measured on a Wallace and Tiernan Series 1500 differential pressure gauge. Quantities of reactants and products were measured by direct weighing or by *PVT* measurements.

IR spectra were taken on a Perkin-Elmer 1430 spectrometer connected to a 3600 data station using a 10-cm gas cell fitted with KCl windows and a glass–Teflon valve. ^{19}F NMR spectra were taken on a Jeol-FX-90Q Fourier transform spectrometer with ~80 mol % CCl_4 as solvent and ~20 mol % $CDCl_3$ as internal lock. $CFCl_3$ was used as an internal

---

(1) Presented in part at the 8th European Symposium on Fluorine Chemistry, Jerusalem, Israel, August 1983; Abstract I-4. Southeastern Regional American Chemical Society Meeting, Charlotte, NC, Nov 1983; Abstract O-422.

(2) Chang, S. C.; DesMarteau, D. D. *Inorg. Chem.* **1983**, *22*, 805.

(3) O'Brien, B. A.; DesMarteau, D. D. *J. Org. Chem.* **1984**, *49*, 1467; *Rev. Chem. Miner.* **1986**, *23*, 621.

(4) Zheng, Y. Y.; DesMarteau, D. D. To be published.

(5) Zheng, Y. Y.; Bauknight, C. W., Jr.; DesMarteau, D. D. *J. Org. Chem.* **1984**, *49*, 3590.

(6) O'Brien, B. A.; Thrasher, J. S.; Bauknight, C. W., Jr.; Robin, M. L.; DesMarteau, D. D. *J. Am. Chem. Soc.* **1984**, *106*, 266.

(7) Ruff, J. K. *J. Org. Chem.* **1967**, *32*, 1675.

(8) Yu, S. L.; Shreeve, J. M. *Inorg. Chem.* **1976**, *15*, 14.

(9) Mir, Q.-C.; DesMarteau, D. D. *J. Fluorine Chem.* **1990**, *48*, 367.

(10) During the course of this work a related but different study on the oxidation of $(CN)_2$ by Br_2 and Cl_2 in the presence of HgF_2 was reported: Waterfeld, A.; Mews, R. *J. Chem. Soc., Chem. Commun.* **1982**, *839*.

0020-1669/91/1330-0535$02.50/0